

RESEARCH ARTICLE

Active Noise Control Scheme for Smart Beds Based on a Wide and Narrow Band Hybrid Control Algorithm

GUOQIANG LU^{1,2}, RENWEN CHEN¹, AND HAO LIU¹¹State Key Laboratory of Mechanics and Control of Mechanical Structures, Nanjing University of Aeronautics and Astronautics, Nanjing 210016, China²School of Electronic and Information Engineering, Sanjiang University, Nanjing 210012, China

Corresponding author: Renwen Chen (bt2101502@nuaa.edu.cn)


ABSTRACT The importance of information intelligence in today's society is growing as a result of advances in science and technology, and as intelligent technology is now a part of almost every aspect of people's lives, demand for data collection technology is rising. The active noise management of smart beds has proven to be a significant difficulty. Smart beds are a type of intelligent function bed that rely on intelligent sensor technologies to perform real-time monitoring of human health and sleep. The active noise control issue for smart beds is addressed in this study, which also suggests an enhanced broadband-narrowband hybrid control method based on the traditional hybrid control technique. In response to the experimental findings, acoustic feedback cancellation technology increased the stability of the control system, lessened algorithmic calculation difficulties, and more effectively neutralised feedback sound. The maximum steady-state noise reduction in the active noise reduction process is 17.7 dB for the improved wide and narrow band hybrid control algorithm and 13.9 dB for the classical wide and narrow band hybrid control algorithm, according to comparisons between time domain sound pressure and linear total sound pressure level results. After active noise reduction, both techniques can successfully eradicate the narrowband sweeping noise component and have a considerable suppressive effect on the broadband noise component. In comparison to the traditional broadband-narrowband hybrid control method, the revised algorithm has a better effect on noise reduction and has a useful use for intelligent applications.

INDEX TERMS Active noise control, wide-and narrow-band hybrid algorithm, intelligent bed, adaptive filtering.

I. INTRODUCTION

All spheres of life have prospered as a result of the advancement of computer network technology and the social economy, but the rise of the intelligent industry stands out. The growth of the Internet has fueled the growth of the intelligent sector, and some intelligent products have proven popular in social settings [1]. The growth of smart homes demonstrates the industry's robust vitality. The rise of the smart home is being driven by the advancement of artificial intelligence on the Internet [2]. The current application of smart beds, however, is limited to hospitals and nursing homes, and generally for manual control, the noise generation also seems

to be uncontrollable [3]. High-quality sleep is crucial to one's health and quality of life because it accounts for around one-third of life [4]. Applications for therapy and detection have emerged quickly among them, considerably enhancing people's quality of life. It has long been a significant area of research in the field of intelligent technology, both domestically and internationally, for the active noise control of intelligent beds [5]. China's skills for independent intelligent field research and development, intelligent design methodologies, and intelligent bed active noise control (ANC) technology have all advanced significantly. Active noise management of intelligent beds is investigated in this paper using linear and non-linear adaptive algorithms, a single broadband active noise cancellation (ANC) method, a single narrowband ANC (NANC) strategy, and a broadband-narrowband hybrid

The associate editor coordinating the review of this manuscript and approving it for publication was Chao-Yang Chen .

ANC algorithm. Single system algorithms typically provide active cancellation only in the relevant frequency bands, with little to no control of low frequency noise in the uncorrelated frequency bands, and only a modest amount of noise reduction in the broadband bands, as well as overall noise reduction. A wideband and narrowband hybrid ANC technique is recommended for efficient control of low frequency broadband noise. Therefore, a wideband and narrowband hybrid ANC method is proposed for the active suppression of the intelligent bed. The first of three main facets of the research is the examination of the ANC algorithm, the unique structural ANC algorithm. According to the spectral properties of the noise reduction object, the ANC algorithms are then split into three categories: broadband ANC (BANC) algorithms, NANC algorithms, and hybrid broadband and NANC algorithms. The second part is a study of classical broadband-narrowband hybrid structured ANC algorithms, and active suppression for both broadband and narrowband noise. For active noise control in smart beds, the feedback-based wide and narrowband hybrid ANC algorithm based on the filtered least mean square (Filtered-X Least mean square, FxLMS) method is merged with a mixture of the feedback structure algorithm and the narrowband trap algorithm. This study's improved wide and narrow band hybrid control algorithm for active noise reduction is tested experimentally, and its performance is compared to that of the classical wide and narrow band hybrid control algorithm and the improved wide and narrow band hybrid control algorithm.

II. RELATED WORKS

Since they were initially developed, ANC techniques have gained prominence as a significant method for reducing low frequency noise in the present. In order to decouple the two structures by using the same adaptive feedback structure reference signal, Wu L. et al. developed a portable ANC pillow that combines a fixed feedback structure with an adaptive feedback structure. The combination of adaptive and fixed feedback systems could improve noise reduction performance, according to experimental results [6]. An algorithm was put forth by Ahmed S. et al. to enhance the FxLMS algorithm's performance when the quadratic path has saturated nonlinearities. The weights of the controller are changed using the suggested manner by minimising a cost function with two terms. After saturation has occurred, it is avoided that the (controller) weights will fluctuate unnecessarily as a result of significant changes in the controller output. Experimental evidence [7] is used to support the method's superiority over other ways in various situations. Huynh M. C. and Chang C. Y. developed a potent non-linear adaptive feedback neural controller that eliminates narrowband noise in both linear and non-linear ANC systems. The method's quick convergence rate, high stability, and efficiency were confirmed by experimental data [8]. An active fault tolerant control (FTC) strategy for temperature control in the combustion zone of cement kilns was proposed by Veerasamy G et al. An Adaptive Kalman Filter (AKF) is

included into the current Model Predictive Control (MPC) framework to accomplish FTC [9]. Using an active and flexible docking technique, Chu W and Huang X have created a big gear structure active and flexible docking system based on distributed force sensors. The approach addresses the issue of the conventional active flexible docking systems' limited load-bearing capability and is practicable [10]. For the purpose to effectively manage wideband active noise, Long G et al. present the design of a subband ANC system. The delay-free subband method's parameter design incorporates genetic algorithm optimisation, and a straightforward near-black-box ANC algorithm optimisation model is created. The use of automatic genetic algorithm optimisation for multi-channel low-frequency broadband active noise reduction systems utilising a delay-free subband algorithm configuration was experimentally verified and shown to be useful [11].

The effectiveness of broadband-narrowband hybrid control algorithms has drawn a lot of interest in the field of active noise reduction. numerous academics have concentrated on the research of broadband-narrowband hybrid control algorithms and have produced numerous impressive research findings. A broadly adjusted graphene liquid crystal photodetector was proposed by Sadeghi H et al. A single layer of graphene on top of a silicon grating makes up the photodetector [12]. The performance of the system was enhanced by simulating autonomous driving decisions under various complex scenarios, according to Guo Z et al.'s construction. The road driving model was created in accordance with the actual needs, and the general architecture of the system and its functional modules were established. The test findings demonstrate that the intelligent decision-making system has some capabilities for decision control and that performance has been significantly enhanced [13]. By using a variable control method in the model predictive control MPC to control the maximum deviation parameter under all non-linear situations, Ali S U et al. offer a distributed MPC-based control technique for multivariate optimisation. Depending on their capabilities, individual controllers will manage the other parameters. The control algorithm's good dynamic response and constraint inclusion were empirically confirmed [14].

In summary, there are still deficiencies in ANC research today, lack of control effects, relatively limited noise reduction bandwidths as well as total noise reduction. Therefore, based on the research aspects of active noise control, new solutions for noise control algorithms for intelligent beds are explored. This study focuses on the effectiveness of an enhanced broad and narrow band hybrid active noise control algorithm for smart beds, which in turn offers a scientific foundation for the development of active control systems.

III. ANC METHOD FOR SB BASED ON WIDE AND NARROW BAND HYBRID CONTROL ALGORITHM

According to the amount of energy dispersion in the frequency band and frequency band, noise in the actual world is

separated into three categories: broadband noise, narrowband noise, and mixed broadband-narrowband noise. According to the frequency range of the noise reduction object, ANC algorithms are classified as BANC algorithms, NANC algorithms, and combined broadband-NANC algorithms [15]. Realising the active control of adaptive following noise is therefore crucial for achieving the necessary control effect on the surrounding sound field.

A. THE ANC APPROACH TO FACING SB

Noise control technology includes two methods: passive control and active control [16]. Passive control technology has a good control effect on high frequency noise, but a poor control effect on low frequency noise. Active noise control technology, on the other hand, uses the principle of acoustic interference cancellation to generate sound waves that have the same frequency and amplitude as the noise source, but in phase opposition, and superimpose them on the noise source to achieve the goal of acoustic noise reduction. The physical basis of active noise control is to achieve noise energy cancellation through the principle of acoustic wave cancellation interference, as shown in Figure 1.

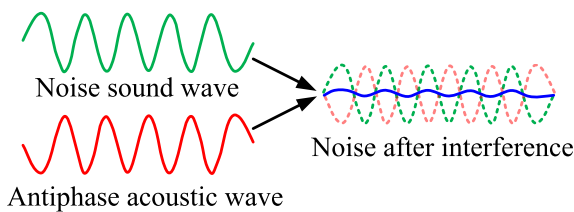


FIGURE 1. Schematic diagram of acoustic wave cancellation interference.

Figure 1 shows acoustic wave interference. When two series of sound waves propagate simultaneously in the same medium, the vibration at any point will cause the superposition of the two vibrations, hence it is called acoustic wave interference. When two series of sound waves propagate to the same position, the occurrence of the same vibration will result in phase interference, but if there is an inverse vibration, there will be destructive interference. The transmission of sound waves causes a particle to generate kinetic energy and potential energy, and the sum of the two is the acoustic energy received by the particle in the acoustic disturbance. The kinetic energy and potential energy of the particle are given by equation (1).

$$\begin{cases} \Delta E_k = \frac{1}{2} m_o v^2 = \frac{1}{2} (\rho_o V_o) v^2 \\ \Delta E_p = - \int_{V_o}^V p dV = \frac{V_o}{2 p_o c_o^2} p^2 \end{cases} \quad (1)$$

In equation (1), p represents the sound pressure, c_o represents the speed of sound wave propagation, V_o represents the volume, ρ_o represents the density and p_o represents the pressure. The sound energy (SE) possessed by the mass is

shown in equation (2).

$$\Delta E = \Delta E_k + \Delta E_p = \frac{1}{2} V_o \rho_o (v^2 + \frac{p^2}{p_o^2 c_o^2}) \quad (2)$$

Equation (3) illustrates that the SE density in a sound field is the SE per unit volume of medium.

$$\varepsilon = \frac{\Delta E}{V_o} = \frac{1}{2} \rho_o (v^2 + \frac{p^2}{p_o^2 c_o^2}) \quad (3)$$

And for planar sound waves, the average SE contained is shown in equation (4).

$$\overline{\Delta E} = \frac{1}{T} \int_0^T \Delta E dt = \frac{1}{2} V_o \frac{p^2}{p_o^2 c_o^2} \quad (4)$$

The SE density of this planar acoustic wave is shown in equation (5).

$$\bar{\varepsilon} = \frac{\overline{\Delta E}}{V_o} = \frac{p^2}{2 p_o^2 c_o^2} \quad (5)$$

Two columns of plane waves satisfying the interference conditions have sound pressures p_1 and p_2 at specific locations in the sound field as shown in equation (6).

$$\begin{cases} P_1 = P_{1\alpha} \cos(\omega t - \varphi_1) \\ P_2 = P_{2\alpha} \cos(\omega t - \varphi_2) \end{cases} \quad (6)$$

In equation (6), $p_{1\alpha}$ and $p_{2\alpha}$ are the sound pressure amplitude of the acoustic wave, ω is the angular frequency of the acoustic wave, φ_1 and φ_2 are the phases of the two columns of acoustic waves, and the phases do not change with time. Equation (7) displays the average SE density of the two sound wave columns.

$$\begin{cases} \bar{\varepsilon}_1 = \frac{P_{1\alpha}^2}{2 \rho_o c_o^2} \\ \bar{\varepsilon}_2 = \frac{P_{2\alpha}^2}{2 \rho_o c_o^2} \end{cases} \quad (7)$$

Equation (8) illustrates how the superposition of sound waves can be used to get the average SE density of the synthetic sound field..

$$\bar{\varepsilon} = \bar{\varepsilon}_1 + \bar{\varepsilon}_2 + \frac{P_{1\alpha} P_{2\alpha}}{\rho_o c_o^2} \cos \varphi \quad (8)$$

In equation (8), φ is the phase difference between the two columns of sound waves, which affects the average SE density at each position in the superimposed sound field, and is calculated as shown in equation (9).

$$\bar{\varepsilon} = \bar{\varepsilon}_1 + \bar{\varepsilon}_2 + \Delta \quad (9)$$

In equation (9), when $P_{1\alpha} = P_{2\alpha}$, $\varphi = \pm n\pi$, $n = 1, 3, 5, 7, \dots$, $\Delta = -\frac{P_{1\alpha} P_{2\alpha}}{\rho_o c_o^2}$, the average SE density of the superimposed sound field is $\bar{\varepsilon} = 0$, which can achieve the phase extinction interference of acoustic waves. The control algorithm is the core issue in active noise control research, as it fundamentally determines the performance of the entire control system. In active noise control systems, the selection

of filters is a very important step. Among them, digital filters are divided into Finite Impulse Response (FIR) and Infinite Impulse Response (IIR) filters. FIR filters do not have the feedback part of the previous output signal and are obtained by weighted summation of the current output signal. The structure of an FIR filter based on the LMS algorithm is shown in Figure 2.

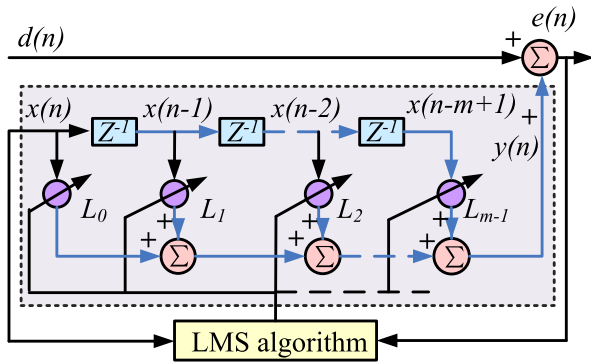


FIGURE 2. FIR filter structure based on lms algorithm.

In Figure 2, the LMS method is utilised to minimise the mean square difference between the output signal and the desired signal in order to dynamically modify the filter weight coefficients. Equation (10), which calculates the filter weight coefficients, is displayed.

$$w(n + 1) = w(n) - 2\mu e(n)x(n) \quad (10)$$

In equation (10), $w(n)$ is the weight coefficient, $e(n)$ is the error signal of the system, and μ is the convergence coefficient. To ensure the stability of the updating process of the weight coefficients, the range of convergence coefficients μ of the LMS algorithm is defined as shown in equation (11).

$$0 < \mu < \frac{1}{tr [R]} \quad (11)$$

In equation (11), $tr [R]$ is the trace of the reference signal autocorrelation matrix R , which is equal to the total power of the input signal, and is defined as shown in equation (12).

$$0 < \mu < \frac{1}{\sum_{i=0}^{L-1} (x(n - i))^2} \quad (12)$$

Because of its short computational cost, the LMS algorithm is frequently employed in adaptive filtering methods. And it was then enhanced to the FxLMS algorithm for use in the active noise field.

B. CHARACTERISATION OF THE STRUCTURAL DIVISION BASED ON THE ANC SYSTEM

Three sections make to the ANC system’s framework. First, based on whether the reference signal is directly acquired or not, feed-forward and feedback ANC systems are differentiated. Second, the ANC system is divided into single-channel

and multi-channel versions depending on how many secondary sources and error microphones are present. Based on the spectral properties of the target noise reduction object, ANC systems are further divided into broadband, narrowband, and wide and NANC systems. In this scenario, the BANC system typically creates a reference noise signal using a reference microphone, resulting in an effective noise reduction of the target noise with noise energy distribution over a broad frequency range. On the other hand, the NANC system is built using non-acoustic sensors. Figure 3 depicts the BANC system and the NANC system.

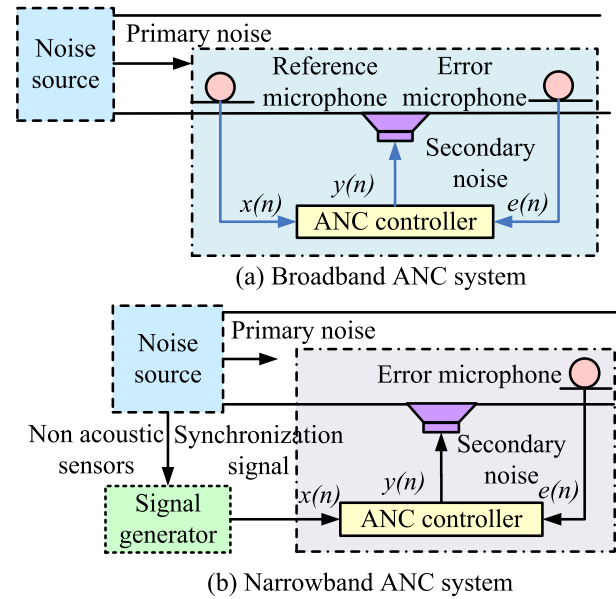


FIGURE 3. Structure diagram of BANC system and NANC system.

In the broadband ANC system shown in Figure 3, in order to achieve the ideal active noise reduction effect for a target noise with noise energy distributed over a wide frequency band, the control system needs to obtain a reference signal that can fully characterize the target noise. The use of a reference microphone can solve this problem. Broadband ANC systems typically use reference microphones as the basis for constructing reference noise signals to achieve effective noise reduction over a wider frequency band [17]. Narrowband ANC systems generate periodic narrowband noise from the movement of mechanical components, which can be supported by non-acoustic sensors to provide more accurate narrowband signals. Even when the microphone is close to the secondary sound source, serious acoustic feedback may occur, but by introducing non-microphones, there is no acoustic feedback problem. It can also effectively track the target noise continuously and has good narrowband order component noise reduction characteristics [18]. Therefore, the broadband and narrowband combined algorithm is superior to both broadband and narrowband algorithms. The hybrid wideband and narrowband ANC system is shown in Figure 4.

Figure 4 shows a wideband and narrowband hybrid ANC system, which has a complex structure compared to

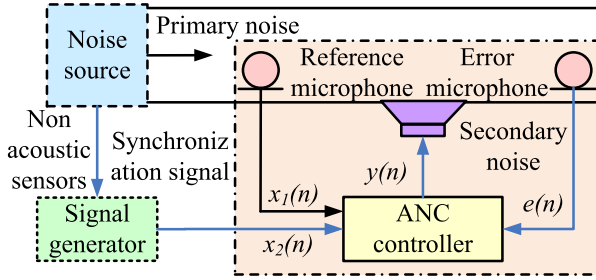


FIGURE 4. Structure diagram of a wide and narrow band hybrid ANC system.

wideband and narrowband algorithm systems. The reference noise signal is constructed using acoustic and non-acoustic microphones, and the offset signal is obtained by summing the output signals of the broadband and narrowband ANC sections. The computational complexity is greater than the sum of the broadband and narrowband algorithms, and targeted processing is performed on the narrowband and broadband components of the mixed broadband and narrowband noise. For noise with mixed characteristics of wide and narrow bands, using a narrow band mixed ANC system composed of a broadband ANC subsystem and a narrow band ANC subsystem is the effective method for handling such noise using active noise control algorithms.

C. IMPROVED WIDE AND NARROW BAND HYBRID CONTROL ALGORITHM BASED ON CLASSICAL WIDE AND NARROW BAND HYBRID CONTROL ALGORITHM

The pre-feedback hybrid ANC algorithm and the wide- and narrow-band hybrid ANC algorithm are the two basic algorithms that make up the wide- and narrow-band hybrid ANC system's hybrid structure. With the goal to provide a more acceptable error signal with two ANC system control filters, a third adaptive filter is added to the traditional pre-feedback hybrid ANC system. As a result, the upgraded system also has faster convergence and greater noise reduction [19]. On this basis, a sinusoidal noise suppressor (SNC) is introduced to coordinate the simultaneous operation of broadband ANC subsystems and narrowband ANC subsystems. The structure of the classic wide narrow band hybrid ANC algorithm is shown in Figure 5.

The classic wideband and narrowband mixed ANC algorithm shown in Figure 5 has a good active suppression effect on common wideband and narrowband mixed noise. The algorithm consists of three parts: wideband ANC system (BANC), narrowband ANC system (NANC), and signal separation system (SNC). This study improves the classic wide and narrow band hybrid ANC system by introducing acoustic feedback cancellation technology to neutralize the collected feedback sound. In order to decrease the degree of algorithm computation, the trapped delay LMS algorithm is implemented in place of the FxLMS method that is utilised in the NANC system. The traditional FxLMS algorithm of the wideband ANC system is then replaced by a normalised

FxLMS algorithm to improve the stability of the control system under impulsive interference. Figure 6 depicts the architecture of the enhanced wideband-narrowband hybrid ANC algorithm.

The improved wide and narrow band hybrid ANC algorithm shown in Figure 6 solves the problem of acoustic feedback cancellation caused by the introduction of a reference microphone. In practical scenarios, the elimination of acoustic feedback can affect the noise reduction performance, making it difficult to fully utilise its power [20]. The number of adaptive notch controllers in the NANC subsystem in the figure increases exponentially with the number of narrowband components to be denoised, but this makes the computation more complex. Therefore, the FxLMS algorithm is replaced by the Notch Delay LMS algorithm to reduce the computational complexity of the algorithm. The wide and narrow band signal after adding acoustic feedback cancellation is separated, and the calculation formula for the feedback acoustic signal is shown in equation (13).

$$x_m(n) = x_R(n) - y_f(n) \quad (13)$$

In equation (13), $y_f(n)$ is the feedback sound signal in the mixing algorithm, $x_R(n)$ is the signal collected by the reference microphone, and $x_m(n)$ is the reference signal after the mid-feed feedback sound. And the broadband noise $x_B(n)$ separated by the improved SNC subsystem is defined as shown in equation (14).

$$x_B(n) = x_m(n) - \sum_{i=1}^q \left[\hat{a}_{si}(n)x_{ai}(n) + \hat{b}_{si}(n)x_{bi}(n) \right] \quad (14)$$

In equation (14), $\left\{ \hat{a}_{si}(n), \hat{b}_{si}(n) \right\}_{i=1}^q$ is the discrete Fourier coefficient of the cosine and sine components, and q is the number of narrowband components to be controlled. The secondary path coefficients and the reference signal no longer need to be convolved, which reduces the operational complexity of the algorithm and allows for the insertion of the trap-delay LMS algorithm. The equation for calculating the adaptive filter weight coefficients in the trap-delay LMS algorithm is shown in equation (15).

$$\begin{cases} \hat{a}_{si}(n+1) = \hat{a}_{si}(n) + \mu_n e(n)x_{ai}(n-d) \\ \hat{b}_{si}(n+1) = \hat{b}_{si}(n) + \mu_n e(n)x_{bi}(n-d) \end{cases} \quad (15)$$

In equation (15), $x_{ai}(n-d)$ and $x_{bi}(n-d)$ are the cosine component reference signal and the sine component reference signal after delaying d samples, respectively. In the normalised FxLMS algorithm, the convergence coefficients are adjusted to adaptively changing time-varying values with the filter weight coefficients shown in equation (16).

$$w(1+n) = \frac{\tilde{\mu}_b}{\delta + x_B^L(n)x_B(n)} e(n)\hat{x}_B(n) + w(n) \quad (16)$$

In equation (16), $\tilde{\mu}_b$ is the base convergence coefficient and δ is a very small positive real number. This study suggests a

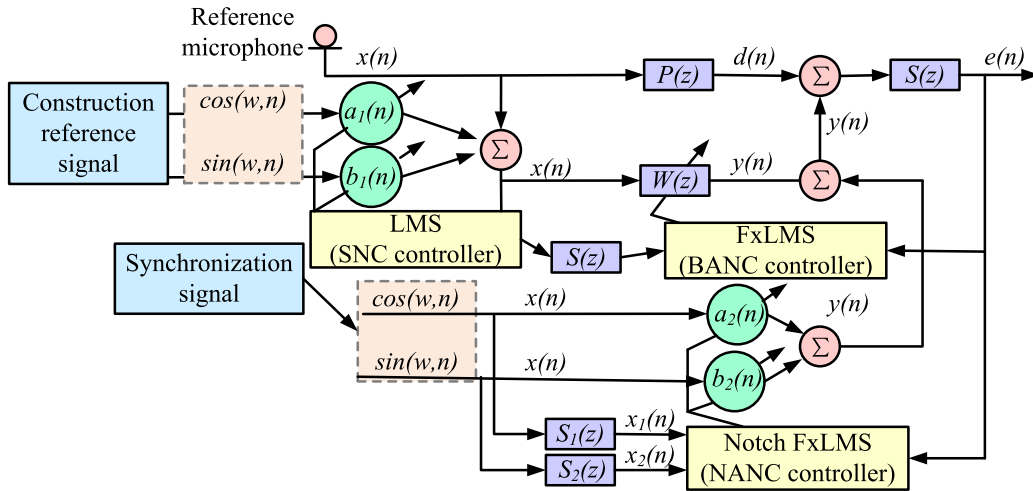


FIGURE 5. Structure diagram of classic wide narrow band hybrid ANC algorithm.

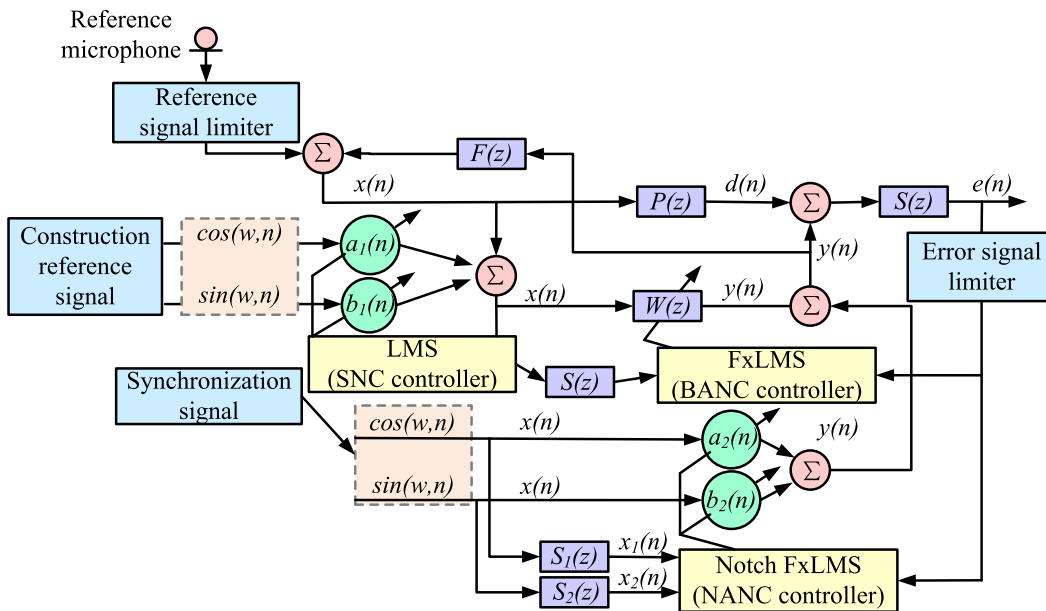


FIGURE 6. Structure diagram of classic wide narrow band hybrid ANC algorithm.

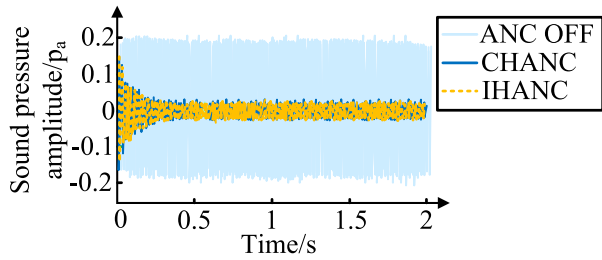
plan to enhance the broadband-narrowband hybrid algorithm in order to further enhance the performance of the ANC algorithm.

IV. ANALYSIS OF SBANC VERIFICATION BASED ON WIDE AND NARROW BAND HYBRID CONTROL ALGORITHM

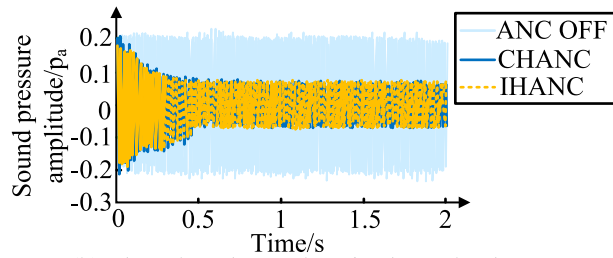
End-to-end speaker-based characterization has strong promise as deep learning emerges as a major technique in the field of intelligent speech and is widely utilised in speaker recognition [19]. Convolutional neural networks cannot directly simulate speaker information between multiple channels while collecting training data from separate channels. Active noise reduction experiments on the Smart Bed (SB) are conducted in this study to evaluate and analyse the

effectiveness of the suggested broad and narrow band hybrid control algorithm for SBANC. This study also proposes an improved ANC hybrid algorithm based on the conventional ANC hybrid algorithm. Figure 7 compares the results for the noise reduction impact between the traditional trapped FxLMS method and the trapped delay LMS algorithm in the scenarios of people going to bed at night and waking up in the morning.

Figure 7 shows the active noise reduction experiments with simulated noise in the morning and evening, using the conventional trapped FxLMS algorithm and the trapped delay LMS algorithm. The time-domain sound pressure amplitude curves for both noise reductions are shown in Figures 7(a) and 7(b), respectively. Figure 7(b) also compares



(a) Time domain results of noise reduction simulation for smart beds during morning hours



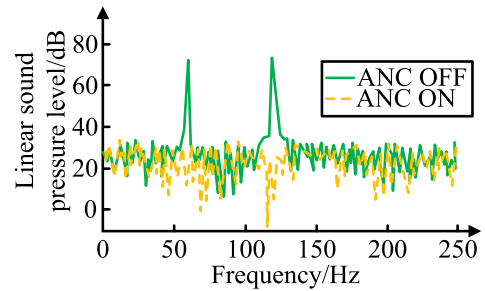
(b) Time domain results of noise reduction simulation for smart beds during the evening period

FIGURE 7. The denoising effect of traditional notch FxLMS algorithm and notch delay LMS algorithm in the morning and evening.

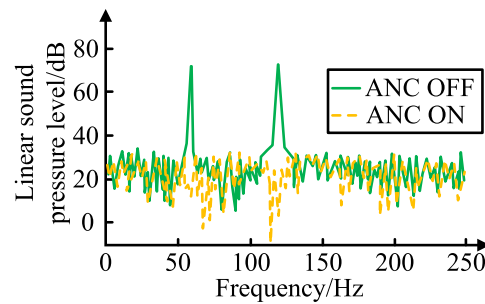
the time-domain total sound pressure level curves for both noise reductions. It is evident that the two algorithms produced similar noise reduction outcomes. Figure 8 displays the results of comparing the steady-state spectra of the two noise reduction techniques.

The steady-state spectra of the two noise reduction outcomes are shown in Figure 8, and they are practically identical in terms of their steady-state noise reduction results. The noise reduction result is the same for second-order noise from 75dB before noise reduction to 13.7dB and 13.6dB, respectively, for the trap-delay LMS algorithm and the traditional trap FxLMS algorithm in the early stage. For fourth-order noise, the noise reduction was almost identical from 75dB before noise reduction to 11.6dB and 11.5dB, respectively. Thus, the trap-delay LMS algorithm's and the traditional trap-FxLMS algorithm's noise-reduction effects in narrowband are essentially equivalent. For the time-frequency analysis, the noise data from 1-4s during the noise reduction process was chosen, and the results are displayed in Table 1.

Table 1 shows that the performance of the trap-delay LMS algorithm and the traditional trap-FxLMS algorithm in terms of noise reduction is very similar. The statistics clearly show that the trap-delay LMS algorithm's noise reduction effect is marginally superior to that of the traditional trap-FxLMS technique, nonetheless. This is because the trap-delay LMS algorithm's computational handling of the secondary filtered reference signal has been eliminated, greatly reducing the algorithm's operational complexity. The active management of narrowband noise is much improved by this. Additionally, a comparison of the anti-pulse performance of the traditional FxLMS method is employed for testing the effectiveness of

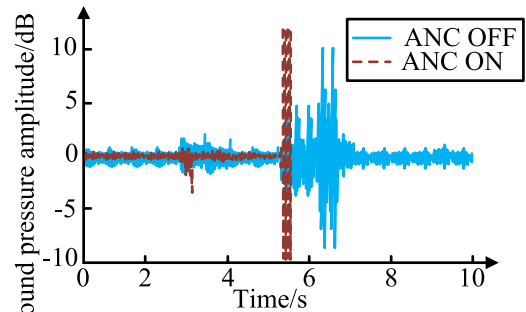


(a) Notch FxLMS algorithm

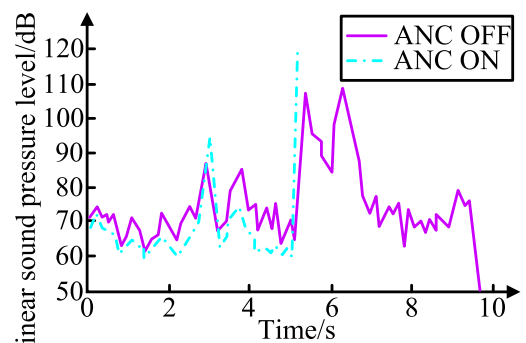


(b) Notch Delay LMS Algorithm

FIGURE 8. Frequency domain results of noise reduction using traditional notch FxLMS algorithm and notch delay LMS algorithm.



(a) Sound pressure amplitude curve



(b) Total sound pressure level curve

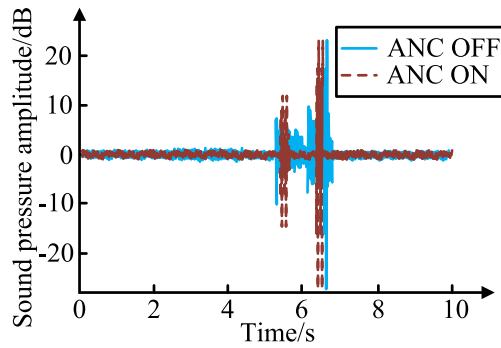
FIGURE 9. Noise reduction performance curve of smart bed under FxLMS algorithm ($\mu = 0.05$).

the suggested improved algorithm for high SPL impulse noise suppression. Figure 9 displays the results of the comparison.

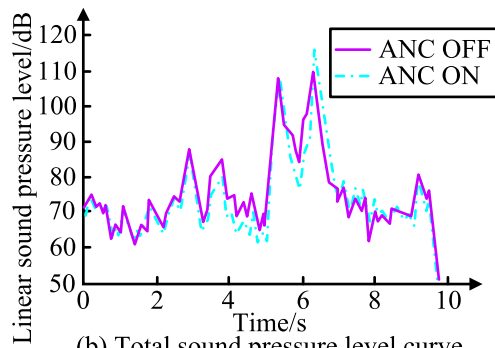
As can be observed from Figure 9, the SB has a good noise reduction control effect on the noise created by contacting the

TABLE 1. Noise reduction time-frequency results of notch FxLMS algorithm and notch delay LMS algorithm.

Time	Before active noise reduction		Notch FxLMS algorithm		Notch Delay LMS Algorithm	
	Frequency	Frequency	Frequency	Linear sound pressure level	Linear sound pressure level	Linear sound pressure level
1	89Hz	72Hz	73Hz	43dB	47dB	40dB
2	116Hz	107Hz	109Hz	57dB	61dB	56dB
3	149Hz	135Hz	137Hz	65dB	72dB	63dB
4	178Hz	167Hz	168Hz	88dB	93dB	87dB



(a) Sound pressure amplitude curve

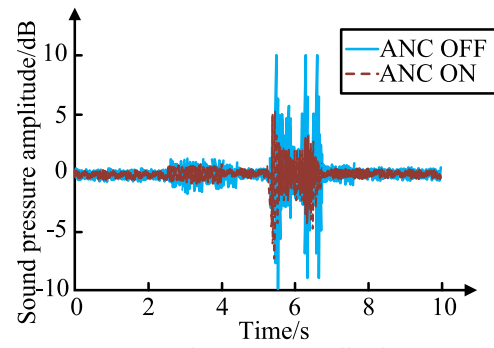


(b) Total sound pressure level curve

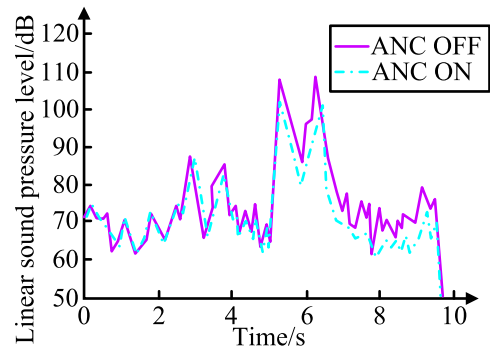
FIGURE 10. Noise reduction performance curve of smart bed under FxLMS algorithm ($\mu = 0.003$).

bed surface with the human body when the algorithm uses a higher convergence factor. However, as the time increases to 5.7s, the noise reduction effect of SB becomes worse, the control system generates divergence, the control process fails and the linear total sound pressure level of SB increases significantly. Therefore, a medium convergence factor was again selected for the experiment. The experimental results are shown in Figure 10.

As demonstrated in Figure 10, SB can guarantee that the noise produced by the human body in contact with the bed has a certain noise reduction effect, although the effect is not significant. This is done by using a medium convergence factor in the FxLMS algorithm. As the time increases to 5.7s, there is still a noise reduction effect and the control system no longer produces dispersion. However, it can be seen from Figure 10(b) that the control effect for high sound pressure impulse noise is poor under this algorithm. The test was then chosen to have a low equal convergence coefficient, and the results are displayed in Figure 11.



(a) Sound pressure amplitude curve



(b) Total sound pressure level curve

FIGURE 11. Noise reduction performance curve of smart bed under FxLMS algorithm ($\mu = 0.001$).

As seen in Figure 11, while using low equal convergence coefficients in the FxLMS algorithm, the noise produced by SB in human contact with the bed has a considerable noise reduction effect. And as time increases, there is still a noise reduction effect, and the control system does not disperse while it has a good control effect on the high sound pressure impulse noise of SB. However, there is a lack of control effect on the noise of the internal structure of the SB. It is obvious that the three possible convergence coefficients for the FxLMS algorithm's noise reduction effect each have flaws. Therefore for the control of SB active noise, the FxLMS algorithm with a fixed convergence factor has obvious limitations. The broadband and NANC subsystems are thoroughly analysed in this paper, which also suggests an enhanced broadband-narrowband hybrid ANC algorithm. Figure 12 provides a detailed comparison of the traditional wide-band hybrid ANC algorithm (CHANC) and the enhanced wide-band hybrid ANC algorithm (IHANC) suggested in this study.

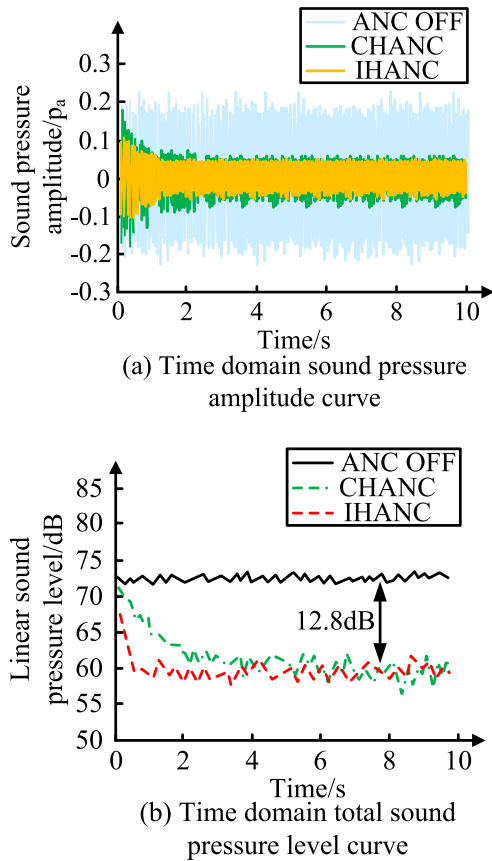


FIGURE 12. Time domain comparison of CHANC algorithm and IHANC algorithm for noise reduction in morning wide and narrow band mixed noise.

Time domain sound pressure and linear total sound pressure level comparison findings are shown in Figures 12(a) and (b), respectively, before and after active noise reduction. As can be seen from the figures, the IHANC algorithm converges faster than the CHANC algorithm in the active noise reduction process. The two algorithms are almost identical in terms of steady-state noise reduction, both achieving an approximate noise reduction of 12.8dB. The noise data from 7-10s of the noise reduction process in the figure was selected for spectral analysis, and the resulting steady-state spectrum in the frequency domain is shown in Figure 13.

The CHANC algorithm lowers the peak sound pressure level at 80Hz from 73.8dB to 32.9dB, a 40.9dB reduction, as seen in Figure 13. The peak sound pressure level at 160Hz is reduced from 67.9dB to 29.3dB, a reduction of 38.6dB, which has a significant noise reduction effect on broadband random noise. The IHANC algorithm reduces the peak noise pressure level at 80Hz from 73.8dB to 31.5dB, a reduction of 42.3dB, while the peak noise pressure level at 160Hz is reduced from 67.9dB to 29.5dB, a reduction of 38.4dB. The results are shown in Figure 14.

Both techniques clearly reduce noise, as shown in Figure 14, as the active noise reduction effect progressively stabilises. The IHANC algorithm's maximum

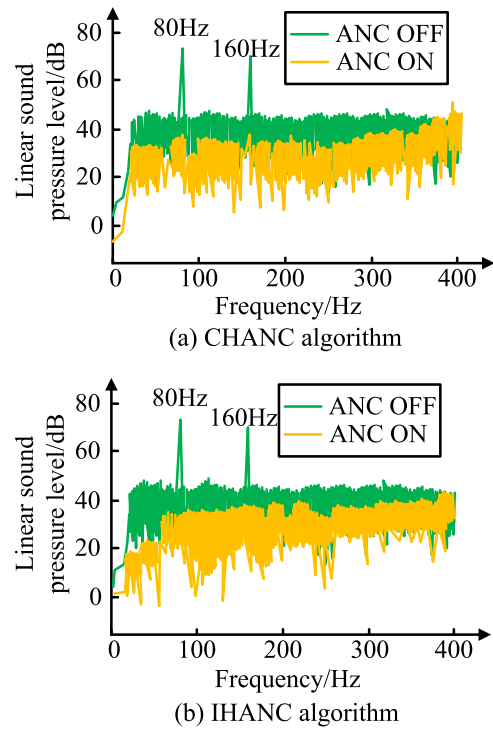


FIGURE 13. Comparison of steady-state spectra between the CHANC algorithm and the IHANC algorithm for morning wide and narrow band mixed noise denoising.

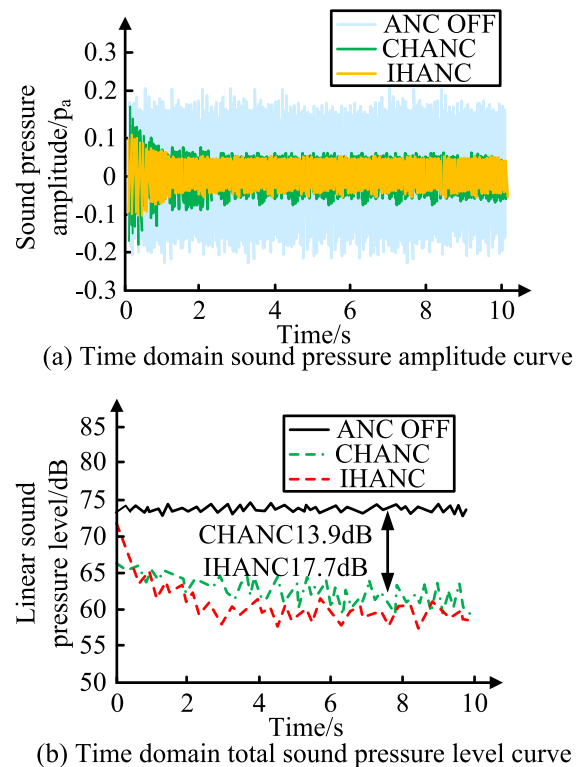


FIGURE 14. Time domain comparison of CHANC algorithm and IHANC algorithm for night wide and narrow band mixed noise reduction.

steady-state noise reduction is 17.7 dB, while the CHANC algorithm's maximum steady-state noise reduction

is 13.9 dB. The IHANC algorithm has a better steady-state noise reduction effect than the CHANC algorithm. Both algorithms have obvious suppression effects on the wide-band noise component, and after active noise reduction, both can effectively eliminate the narrowband swept noise component. This shows that the IHANC algorithm has a better noise reduction effect than the CHANC algorithm.

V. CONCLUSION

SBANC technology has advanced significantly as a result of the ongoing advancement of intelligent technology and intelligent design methodologies. This study investigates whether ANC can be applied to and improved for the wide and narrow band hybrid noise present in SB, suggests an improved wide and narrow band hybrid control algorithm based on the active noise control algorithm, and tests the algorithm's efficacy using experiments. According to the experimental findings, the traditional trap FxLMS method and the trap delay LMS strategy both had equivalent noise reduction effects for second-order noise, which was reduced from 75 dB before noise reduction to 13.7 dB and 13.6 dB, respectively. The noise reduction for fourth-order noise was nearly equal, going from 75 dB before noise reduction to 11.6 dB and 11.5 dB, respectively. The noise reduction impact of SB degrades, the control system causes divergence, the control procedure fails, and the linear total sound pressure level of SB dramatically rises when the FxLMS algorithm uses a larger convergence factor. When using medium convergence coefficients, the FxLMS algorithm reduces some noise, but the effect is minimal, and the control system no longer produces divergence. Low convergence coefficients significantly reduce noise when using the fxLMS algorithm. And as time passes, there is still a noise reduction effect. The SB's high sound pressure impulse noise is well controlled by the control system without divergence, however the SB's internal structure noise is not well controlled. This demonstrates that the FxLMS method fails to effectively reduce noise for each of the three convergence factors. The FxLMS approach with fixed convergence coefficients, then, has apparent limits for the management of SB active noise. This paper offers a thorough examination of the ANC subsystems for both broadband and narrowband, and it suggests an enhanced hybrid ANC algorithm for both. A thorough comparison is made between the enhanced wide-band hybrid ANC algorithm (IHANC) suggested in this study and the traditional wide-band hybrid ANC algorithm (CHANC) in terms of noise reduction performance. The IHANC method converges more quickly than the CHANC algorithm during active noise reduction. Overall, the two achieve roughly a 12.8dB noise reduction in steady-state operation, making them nearly similar. The IHANC algorithm reduces noise by 42.3 dB at 80 Hz and 38.4 dB at 160 Hz, but the CHANC approach only achieves 40.9 dB at 80 Hz and 38.6 dB at 160 Hz. In terms of noise reduction and convergence, the IHANC algorithm outperforms the CHANC approach. The IHANC algorithm has a maximum steady-state noise reduction of 17.7 dB, whereas the CHANC

algorithm has a maximum steady-state noise reduction of 13.9 dB once the active noise reduction impact has gradually stabilised. After active noise reduction, both techniques can successfully eradicate the narrowband sweeping noise component and have a considerable suppressive effect on the broadband noise component. It is clear that the IHANC algorithm reduces noise more effectively than the CHANC method does. The theoretical underpinnings of this research are solid and scientific, but there hasn't been any experimental investigation of its practical applicability in real life, therefore the approach needs more testing in actual applications.

REFERENCES

- [1] C. Gong, M. Wu, J. Guo, Z. Zhang, Y. Cao, and J. Yang, "Multichannel narrowband active noise control system with a frequency estimator based on DFT coefficients," *J. Sound Vib.*, vol. 521, Mar. 2022, Art. no. 116660, doi: [10.1016/j.jsv.2021.116660](https://doi.org/10.1016/j.jsv.2021.116660).
- [2] J. Liu and Z. Wang, "A narrowband active noise control system with autoregressive model and linear cascaded adaptive notch filter," *Signal Process.*, vol. 196, Jul. 2022, Art. no. 108502, doi: [10.1016/j.sigpro.2022.108502](https://doi.org/10.1016/j.sigpro.2022.108502).
- [3] W. Chen, H. Williams, C. Lu, Z. Liu, and Y. Sun, "Development and experimental verification of a new computationally efficient parallel narrowband active noise control system," *Appl. Acoust.*, vol. 187, Feb. 2022, Art. no. 108510, doi: [10.1016/j.apacoust.2021.108510](https://doi.org/10.1016/j.apacoust.2021.108510).
- [4] C. Y. Chang, C. T. Chuang, S. M. Kuo, and C. H. Lin, "Multi-functional active noise control system on headrest of airplane seat," *Mech. Syst. Signal Process.*, vol. 167, Mar. 2022, Art. no. 108552, doi: [10.1016/j.ymsp.2021.108552](https://doi.org/10.1016/j.ymsp.2021.108552).
- [5] H. Huang, "Graphene-silver hybrid metamaterials for tunable narrow-band perfect absorption and reflection at visible waveband," *J. Nanophotonics*, vol. 15, Apr. 2021, Art. no. 026005, doi: [10.1117/1.JNP.15.026005](https://doi.org/10.1117/1.JNP.15.026005).
- [6] L. Wu, F. Niu, and Y. Guo, "Active noise control pillow based on the combination of the fixed and adaptive feedback structures," *Appl. Acoust.*, vol. 185, Jan. 2022, Art. no. 108396, doi: [10.1016/j.apacoust.2021.108396](https://doi.org/10.1016/j.apacoust.2021.108396).
- [7] S. Ahmed, M. Tufail, M. Rehan, T. Abbas, and A. Majid, "A novel approach for improved noise reduction performance in feed-forward active noise control systems with (loudspeaker) saturation non-linearity in the secondary path," *IEEE/ACM Trans. Audio, Speech, Language Process.*, vol. 29, pp. 187–197, 2021, doi: [10.1109/TASLP.2020.3039607](https://doi.org/10.1109/TASLP.2020.3039607).
- [8] M.-C. Huynh and C.-Y. Chang, "Nonlinear neural system for active noise controller to reduce narrowband noise," *Math. Problem Eng.*, vol. 2021, May 2021, Art. no. 5555054, doi: [10.1155/2021/5555054](https://doi.org/10.1155/2021/5555054).
- [9] G. Veerasamy, R. Kannan, R. Siddharthan, G. Muralidharan, V. Sivanandam, and R. Amiratharan, "Integration of genetic algorithm tuned adaptive fading memory Kalman filter with model predictive controller for active fault-tolerant control of cement kiln under sensor faults with inaccurate noise covariance," *Math. Comput. Simul.*, vol. 191, pp. 256–277, Jan. 2022, doi: [10.1016/j.matcom.2021.07.023](https://doi.org/10.1016/j.matcom.2021.07.023).
- [10] W. Chu and X. Huang, "An active compliant docking method for large gear components based on distributed force sensor," *Sensor Rev.*, vol. 42, no. 3, pp. 303–315, May 2022, doi: [10.1108/SR-08-2021-0262](https://doi.org/10.1108/SR-08-2021-0262).
- [11] G. Long, Y. Wang, and T. C. Lim, "Optimal parametric design of delayless subband active noise control system based on genetic algorithm optimization," *J. Vib. Control*, vol. 28, nos. 15–16, pp. 1950–1961, Aug. 2022, doi: [10.1177/10775463211001625](https://doi.org/10.1177/10775463211001625).
- [12] H. Sadeghi, V. Talebi, and H. Soofi, "Ultra-narrow band widely tunable photodetector based on a graphene-liquid crystal hybrid structure," *Opt. Commun.*, vol. 515, Jul. 2022, Art. no. 128214, doi: [10.1016/j.optcom.2022.128214](https://doi.org/10.1016/j.optcom.2022.128214).
- [13] Z. Guo, D. Sun, and L. Zhou, "Research on integrated decision control algorithm for autonomous vehicles under multi-task hybrid constraints in intelligent transportation scenarios," *J. Circuits, Syst. Comput.*, vol. 31, no. 7, May 2022, Art. no. 2250122, doi: [10.1142/S0218126622501225](https://doi.org/10.1142/S0218126622501225).

- [14] S. U. Ali, M. Aamir, A. R. Jafri, U. Subramaniam, F. Haroon, A. Waqar, and M. Yaseen, "Model predictive control—Based distributed control algorithm for bidirectional interlinking converter in hybrid microgrids," *Int. Trans. Electr. Energy Syst.*, vol. 31, no. 10, Oct. 2021, Art. no. e12817, doi: [10.1002/2050-7038.12817](https://doi.org/10.1002/2050-7038.12817).
- [15] M. E. C. Bento, "A hybrid particle swarm optimization algorithm for the wide-area damping control design," *IEEE Trans. Ind. Informat.*, vol. 18, no. 1, pp. 592–599, Jan. 2022, doi: [10.1109/TII.2021.3054846](https://doi.org/10.1109/TII.2021.3054846).
- [16] M. J. Fotuhi and Z. Bingul, "Novel fractional hybrid impedance control of series elastic muscle-tendon actuator," *Ind. Robot*, vol. 48, no. 4, pp. 532–543, Aug. 2021, doi: [10.1108/IR-10-2020-0236](https://doi.org/10.1108/IR-10-2020-0236).
- [17] D. Yang, Y. Shang, Y. Han, W. Li, J. Wu, and B. Niu, "Ultra-thin muffler with coherent coupling weak resonance for HVDC converter station medium frequency band noise control," *IOP Conf. Ser. Earth Environ. Sci.*, vol. 772, no. 1, Mar. 2021, Art. no. 012031, doi: [10.1088/1755-1315/772/1/012031](https://doi.org/10.1088/1755-1315/772/1/012031).
- [18] R. Sepehrzad, M. E. Hassanzadeh, A. R. Seifi, and M. Mazinani, "An efficient multilevel interconnect control algorithm in AC/DC micro-grids using hybrid energy storage system," *Electr. Power Syst. Res.*, vol. 191, Feb. 2021, Art. no. 106869, doi: [10.1016/j.epsr.2020.106869](https://doi.org/10.1016/j.epsr.2020.106869).
- [19] S. Choudhuri, S. Adeniyi, and A. Sen, "Distribution alignment using complement entropy objective and adaptive consensus-based label refinement for partial domain adaptation," *Artif. Intell. Appl.*, vol. 1, no. 1, pp. 43–51, Jan. 2023, doi: [10.47852/bonviewaia2202524](https://doi.org/10.47852/bonviewaia2202524).
- [20] F. Masood, J. Masood, H. Zahir, K. Driss, N. Mehmood, and H. Farooq, "Novel approach to evaluate classification algorithms and feature selection filter algorithms using medical data," *J. Comput. Cogn. Eng.*, vol. 2, no. 1, pp. 57–67, May 2022, doi: [10.47852/bonviewjce2202238](https://doi.org/10.47852/bonviewjce2202238).



RENWEN CHEN received the B.S., M.S., and Ph.D. degrees in test and measurement technology and instrumentation from the Nanjing University of Aeronautics and Astronautics, Jiangsu, China, in 1988, 1991, and 1999, respectively.

He is currently a Postgraduate Tutor with the School of Aeronautics, Nanjing University of Aeronautics and Astronautics. His current research interests include active noise control, machine vision, artificial intelligence, measurement and control technology, energy recovery, and intelligent structures.



GUOQIANG LU was born in Jiangsu, China, in 1981. He received the B.S. degree in electronic science and technology from Southeast University, Jiangsu, in 2005, and the M.S. degree in instrument science and technology from the Nanjing University of Aeronautics and Astronautics, Jiangsu, in 2008, where he is currently pursuing the Ph.D. degree in instrument science and technology.

His current research interests include active noise control, machine vision, and measurement and control technology.



HAO LIU received the M.S. degree in electronics and communication engineering from North University, Taiyuan, China, in 2021. He is currently pursuing the Ph.D. degree in instrument science and technology with the Nanjing University of Aeronautics and Astronautics. His current research interests include optimization theory, UAV formation, and wireless sensor networks.

• • •